JOURNAL OF Applied Polymer SCIENCE

Neural network modeling of the preparation process of a siloxane-organic polyazomethine

Ioan Florin Macsim,[1] Elena Niculina Dragoi,[1] Maria Cazacu,[2] Silvia Curteanu[1]

[1]"Gheorghe Asachi" Technical University Iasi, Department of Chemical Engineering and Environmental Protection, Bd. Prof.dr.doc. Dimitrie Mangeron, No. 71A, 700050, Iasi, Romania

[2]"Petru Poni" Institute of Macromolecular Chemistry, Aleea Gr. Ghica Voda 41A, Iasi, Romania

Correspondence to: S. Curteanu (E-mail: silvia_curteanu@yahoo.com)

ABSTRACT: Although apparently simple, the polycondensation reaction leading to polyazomethine is difficult to control because of its equilibrium character, the conversion degree being influenced by a series of parameters. The reaction between a siloxanediamine, 1,3-bis(3-aminopropyl)tetramethyldisiloxane, and terephthalaldehyde was performed here in solution (in tetrahydrofuran) without by-products removal and in absence of any catalyst or pH modifier. Different conditions (co-monomers ratio, dilution, and temperature), considered as input parameters for the process modeling, were varied according to a pre-established experimental program. The viscosity of the reaction mixture was chosen as output parameter, being monitored with a Haake Viscotester 7 Plus-L. The process modeling was performed using a hybrid combination of artificial neural networks and differential evolution algorithm, the last one having the role of developing the neural model in an optimal form. The simulation results showed that the methodology provides accurate results, the model predictions being in close correlation with the experimental data. © 2015 Wiley Periodicals, Inc. J. Appl. Polym. Sci. **2015**, *132*, 42552.

KEYWORDS: polycondensation; theory and modeling; viscosity and viscoelasticity

Received 17 February 2015; accepted 30 May 2015

DOI: 10.1002/app.42552

INTRODUCTION

Polyazomethines, polyamines, or Schiff base polymers are a class of compounds containing azomethine (C═N) groups obtained by nucleophilic addition of diamines to carbonyl groups of dialdehydes or diketones.[1,2] The structure of the polyazomethines can be easily tailored with fully aromatic, aliphatic, or mixed structure.[1] In general, aromatic co-monomers are used because the derived polyazomethines constitute an attractive class of high performance polymers[3,4] with interesting properties, which are associated mainly with their conjugated backbone and the presence of imine groups: good thermal stability, mechanical strength, nonlinear optical properties, semiconducting properties, environmental stability, and fiber-forming properties, but also ability to form metal chelates.[5–8] Therefore, aromatic polyazomethines are recommended candidates for potential applications in electronics, optoelectronics, and photonics.[9–11] Because of azomethine group, capable of protonation and complexation,[12] Schiff bases are well-known ligands in the transition metal coordination chemistry.[2] Therefore, they were intensely explored.[13]

However, because of the backbone rigidity, the full aromatic polyazomethines show poor solubility in organic solvents and high melting points which limit their practical applications in various fields. Several alternative synthetic strategies such as creation of the molecular asymmetry by incorporating of non-coplanar groups in the main chain, attaching the bulky pendant groups, for instance, the introduction of substituents (alkyl or alkoxy groups) in the ortho-position of the aromatic ring or insertion of aliphatic flexible spacers between aromatic rings within the main chain are approached.[7,8,14–16] Various modified polyazomethines such as poly(azomethine-ester)s, poly(azomethine-ether)s, poly(azomethine-carbonate)s, poly (amide–azomethine-ester)s, poly(acrylate-azomethine)s, thermosetting polyazomethines, poly(azomethine-sulfone)s, poly (azomethine–ether-sulfone)s were also synthesized with the goal to reduce the melting temperature, to improve the solubility, as well as to promote specific properties.[4,17] The inclusion of polyazomethines in rotaxane architecture is another strategy approached to improve their processability.[18] Siloxane moiety had also inserted as a flexible spacer, either in the amine or carbonyl component, resulting in polyazomethines with improved solubility[19–25] because of high flexibility of the siloxane bond and weak intermolecular interactions between dimethylsiloxane units.

In general, polyazomethines are easily obtained, the synthesis requiring mild conditions (without precious catalyst, pressure, or extreme temperature).[12] The only by-product is water and purification of the reaction product is relatively simple.[26] Shifting the equilibrium of this reaction toward the polyazomethine formation is usually favored by the removal of water by-product either by azeotrope distillation or by the use of dehydrating agent (molecular sieves, magnesium sulfate, etc.). The mechanism of polyazomethine formation consists in nucleophilic addition of the amine to the carbonyl group to give in a first stage carbinolamine, an unstable addition compound. Subsequently, this loses water in a rate-determining step of the reaction. Because the carbinolamine is an alcohol, it undergoes acid-catalyzed dehydration. But the acid concentration cannot be too high because amine, being a basic compound, can be protonated and becomes non-nucleophylic and the equilibrium might shift to the left with carbinolamine re-formation. Thus, although apparently simple one, the polycondensation reaction leading to polyazomethine is difficult to control because it is an equilibrium reaction and the conversion degree is influenced by many parameters such as the ratio between the two co-monomers, the presence of by-product (water in this case) in the reaction medium, the temperature, and dilution. The process for the formation of azomethine is pH sensitive.[27]

Real-time measurements of reaction occurrence could provide direct information about the processes or reactions, and are useful in control, optimization, and other decision-making steps. This involves sampling, pretreatment, measurement, interpretation, and application of data.[28] In the course of polymer formation, the rheological parameters of the reactive mass changes and their measurement and analysis could permit to obtain information about the process. However, it is very difficult technically to measure the whole complex of rheological parameters in the course of the process, especially if it is one fast. Therefore, it is preferable to restrict the use of relatively simple methods of viscometric measurements and dynamic analysis, which constitutes the two major groups of methods used nowdays in rheokinetics. The sphere of their application is mainly determined by the properties of the material under study.[29] If the process of polymerization is a relatively low-viscous liquid, viscometric method is recommended for monitoring of the viscosity changes during the chemical process. The monitoring can be carried out through different viscometric techniques available or by using specially designed instruments (capillary or rotational viscometers or vibration instruments), but the parameter to be measured is, in any case, the viscosity of the medium.[29]

The synthesis of a siloxane-organic polyazomethine in solution, in the absence of any catalyst, by *in situ* measurement of the reaction mixture viscosity, was modeled using a procedure based on Artificial Neural Networks (ANNs) and Differential Evolution (DE) algorithm. Using this simulation method, the viscosity of the reaction mixture was correlated with working conditions (co-monomers ratio, dilution, and temperature).

ANNs are inspired from the biological brain and have computational structures capable of modeling complex systems, especially when they are hard to be described mathematically.[30] Also, ANNs can perform parallel processing, learning, and they are fault tolerant. Therefore, ANNs can be efficiently used to solve difficult complex and nonlinear problems, from different areas, their applications including: pattern recognition (automated recognition of hand-written text, fingerprint identification), speech recognition, monitoring, and control of complex plants.[31] In the chemical engineering area, and especially for the polymerization processes, ANNs were applied to a diversity of processes, being included in various methodologies. Some examples are enumerated: direct an inverse modeling of free radical polymerization of methyl methacrylate,[32] development of a virtual soft sensor in the polyethylene terephthalate production process,[33] modeling the styrene living radical polymerization mediated by 2,2,6,6-tetramethyl-1-piper-idinoxyl,[34] selection of mixture initiators for batch polymerization,[35] modeling the free radical polymerization of styrene,[36] reaction temperature prediction during the styrene polymerization,[37] fluorescence modeling of the polydimethylsiloxane/silica composites containing lanthanum[38] and the list remains opened.

DE, on the other hand, is an optimization techniques belonging to the Evolutionary Algorithms (EAs) class, being inspired from the Darwinian principle of evolution, in which only the fittest individuals survive to the next generations. Among all EAs, DE distinguishes as an efficient approach, easy to implement, requiring little parameter tuning, and exhibiting fast convergence.[38] It was applied to solve different types of problems (engineering, scheduling, decision-making, control, image processing) from different areas (chemical engineering, bioinformatics, computational chemistry, molecular biology).[39] For the polymerization processes, DE was applied for optimization of styrene production by dehydrogenation of ethyl benzene in an adiabatic reactor,[40] optimization of two styrene reactor configurations,[41] model optimization for the styrene polymerization process,[36] etc.

In this work, a combination between DE and ANNs is applied for the synthesis of a polyazomethinecontaining flexible siloxane sequences along the chain. DE, in a hybridized form, has the role of optimizing the ANN which acts as a model for the process. In this manner, the best model of the system is determined. This approach, belonging to the neuro-evolutive class, was applied for developing the optimal model because, although simple and easy to work with, ANNs are difficult to setup. Initially, a direct feed forward system was tested, but the results were not in acceptable range and, therefore, a simple recurrence (simulated through data manipulation) was employed to reduce the error of the model.

The rest of this article is organized as follows. Section 2 is reserved to the experimental setup, where materials, equipment, and procedure are described. In the Section 3, the modeling approach is described in details. Information about the algorithm, how the combination algorithm–process is realized, and the data processing procedure are presented. The results and discussion related to the performance of the developed models are included in the Section 4. Section 5 concludes the article.

EXPERIMENTAL

Materials

1,3-Bis(3-aminopropyl)tetramethyldisiloxane (AP0), $[H_2N(CH_2)_3(CH_3)_2Si]_2O$, was purchased from Fluka: b.p. = 142°C/11.5 mmHg, $d_{20}^4 = 0.901$.

Terephthalaldehyde (AT), $C_8H_6O_2$, assay, mp 114 − 116°C (Aldrich).

Tetrahydrofuran (THF), anhydrous, ≥ 99.9%, inhibitor-free (Sigma-Aldrich).

Equipment

The experimental installation (Figure 1) consists in an automatic rotational viscometer, a water bath, and a computer.

The viscometer, a Haake Viscotester 7 Plus-L, was used with small volume reactor and a TL-5 spindle due the low viscosity of the probes. This combination was used because:

- Haake Viscotester 7 Plus-L is able to provide online monitoring of the reaction process and can record the viscosity second by second. For the temperature observation it was used the PT100 temperature sensor.
- The small capacity reactor consists of dish with a reaction volume of 8 mL optimal and is equipped with a thermostatic jacket. It was chosen for its low reagent consumption.
- TL5 spindle has the ability to determine viscosity between 1 and 13.5 mPas, if it is used with the low volume reactor at a rotation speed of 200 rot/min.
- The water bath is a Lauda Ecoline 003, a simple and precise water bath who has an operating temperature range between 25°C and 120°C.
- The computer is connected to the viscometer by a data cable and runs the HAAKE RheoWin suite version 4.20.0005. For the determination of viscosity it has been used the method of CR viscosity time tests in HAAKE RheoWin 4 JobManager, which applies a constant rotation speed to the spindle and monitors the viscosity as a function of time. For data processing, it was used HAAKE RheoWin 4 DataManager.

Fourier transform infrared (FT-IR) spectra were recorded using a Bruker Vertex 70 FT-IR spectrometer in the transmission mode, in the range of 400–4000 cm^{-1} at room temperature, with a resolution of 2 cm^{-1} and an accumulation of 32 scans.

Procedure

AT and AP0 were mixed in different ratios and at various dilutions in THF, directly in the reactor of the viscometer and the reaction mixtures were thermostated at temperature established according to the experimental program (Table I). The progress of reaction was studied by *in situ* continuously measurements of the reaction mixture viscosity by using an automatic viscometer. The product at the end of each experiment was analyzed by spectral technique (FTIR).

The water by-product was not removed from the reaction mixture, the reactions being carried on in conditions in which, depending on the allocated time, as well as the reactants ratio and their reactivity, they can achieve the equilibrium. To continuously measure, *in situ*, viscosity changes, we drove these reactions directly in the viscometer vessel, which, as it is built, does not offer the possibility of removing secondary product as it is formed. The use of drying agents may influence viscosity values. Therefore, we performed the modelling on the basis of other parameters: reactants ratio, solution concentration and temperature, in the presence of by-product.

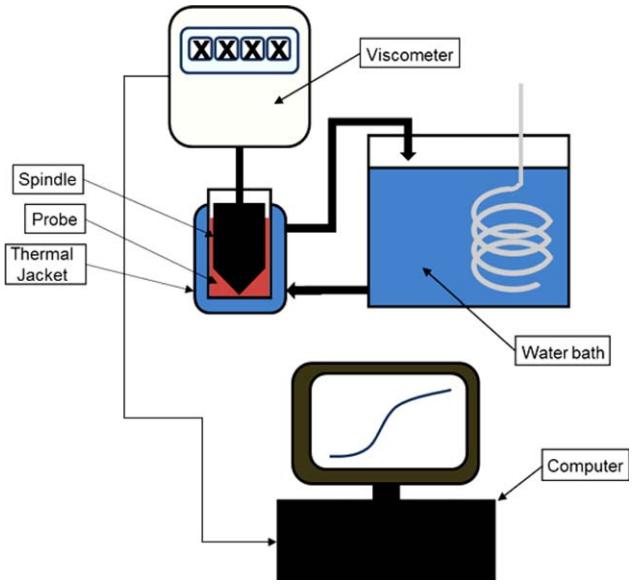

Figure 1. The experimental setup for the monitoring of the condensation reaction. [Color figure can be viewed in the online issue, which is available at wileyonlinelibrary.com.]

A total of 90 experiments consisting in polycondensation reactions at three different concentrations, 15, 20, and 25 wt %, six different temperatures, 25°C, 30°C, 35°C, 40°C, 45°C, and 50°C, and five different co-monomers ratios, 0.5/1, 0.75/1, 1/1, 1/0.75, and 1/0.5 were performed. Some of them could not be monitored, because their viscosity is too low for the reactor/spindle/rotation speed combination that was used. Thus, only 67 remained valid experiments, and they have been included in Table I and further used in modelling.

Operating Model

An experimental program consisting in a matrix with 67 experiments performed in different conditions was established at the beginning (Table I). Co-monomers molar ratio, their concentration in THF (C), and temperature (T) were chosen as input parameters, while viscosity of the reaction mixture was the output parameter.

In order to explain the operating mode, the following conditions were taken into consideration: temperature of 25°C, concentration of 25 wt %, and a 1 : 1 co-monomers molar ratio.

The proper amounts of AT (0.7 g) were dosed and dissolved in 6.56 mL THF in the recipient from the small volume reactor. After this, the recipient was mounted in the thermal jacket and then on the viscometer. The water bath was already settled to 25°C and connected to the thermal jacket. The spindle was immersed in the sample and let to rotate 10 minutes in order to help the solution reach the desired temperature. After 10

Table I. Experimental Matrix

Exp. No.	AT : AP0 (molar ratio)	Conc., (wt/100)[a]	Temp. (°C)	Exp. No.	AT : AP0 (molar ratio)	Conc., (wt/100)[a]	Temp. (°C)
1	2 : 1	15	25	35	3 : 4	20	30
2	2 : 1	15	30	36	3 : 4	20	35
3	4 : 3	15	25	37	3 : 4	20	40
4	4 : 3	15	30	38	3 : 4	20	50
5	4 : 3	15	50	39	1 : 2	20	25
6	1 : 1	15	25	40	1 : 2	20	30
7	1 : 1	15	30	41	1 : 2	20	35
8	1 : 1	15	35	42	1 : 2	20	40
9	1 : 1	15	40	43	1 : 2	20	50
10	1 : 1	15	45	44	2 : 1	25	25
11	1 : 1	15	50	45	2 : 1	25	30
12	3 : 4	15	25	46	2 : 1	25	35
13	3 : 4	15	30	47	2 : 1	25	50
14	3 : 4	15	35	48	4 : 3	25	25
15	3 : 4	15	40	49	4 : 3	25	30
16	3 : 4	15	50	50	4 : 3	25	35
17	1 : 2	15	25	51	4 : 3	25	40
18	1 : 2	15	30	52	4 : 3	25	50
19	1 : 2	15	35	53	1 : 1	25	25
20	1 : 2	15	50	54	1 : 1	25	30
21	2 : 1	20	25	55	1 : 1	25	35
22	2 : 1	20	30	56	1 : 1	25	40
23	2 : 1	20	50	57	1 : 1	25	45
24	4 : 3	20	25	58	1 : 1	25	50
25	4 : 3	20	30	59	3 : 4	25	25
26	4 : 3	20	35	60	3 : 4	25	30
27	4 : 3	20	50	61	3 : 4	25	35
28	1 : 1	20	25	62	3 : 4	25	40
29	1 : 1	20	30	63	3 : 4	25	50
30	1 : 1	20	35	64	1 : 2	25	25
31	1 : 1	20	40	65	1 : 2	25	30
32	1 : 1	20	45	66	1 : 2	25	35
33	1 : 1	20	50	67	1 : 2	25	50
34	3 : 4	20	25				

[a] Total weight of reactants/weight of solution, $C = 100(m_{AP0}+m_{AT}/(m_{AP0}+m_{AT}+m_{THF})$.

minutes have passed, 1.44 mL AP0 were added and the viscometer was started from the program. Evolution of the viscosity of reaction mixture within 3 hours is shown in Figure 2.

IR spectra of the reaction mixture were recorded after solvent evaporation.

MODELING PROCEDURE

Data Gathering and Processing

After the data were gathered using the system described previously, a set of data processing techniques were employed in order to prepare them for the modeling and optimization procedures. These techniques include: (i) elimination of duplicate data; (ii) shuffling; (iii) splitting, and (iv) normalization.

Depending on the reaction speed and frequency of data sampling in the available data, the same system parameters are obtained at different moments of time. In order to reduce the data dimension so that the modeling and optimization procedures run at an optimal speed (which depends not only on the computer power, but also on the process and data dimension), the samples in which only the time is different (the other parameters remaining unchanged) are automatically removed using a simple algorithmic procedure. In this manner, only the significant data will be used for generating the process model.

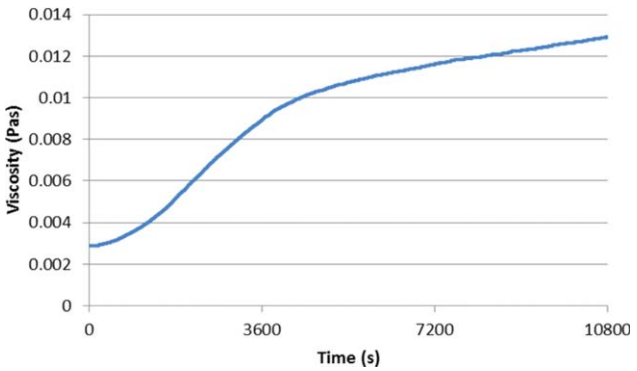

Figure 2. The rheogram obtained for $C = 25\%$, $T = 25°C$ and AP0 : AT molar ratio 1 : 1. [Color figure can be viewed in the online issue, which is available at wileyonlinelibrary.com.]

In order to determine the best ANN that can work as a model for the considered process, the available data must be shuffled and split into two parts - training and testing. Shuffling is performed for avoiding overfitting and preventing the model from learning the data order instead of the actual relationships. On what concerns the data splitting, usually 75% is chosen for training, while the remaining 25% is used for testing. Another consideration for using this splitting is based on several previous tests that show that no significant improvement is obtained with other percentages. This is valid for the current process.

Another approach used for the obtaining of better results is data normalization. In literature, different types of normalizations are encountered; in this work a Min-Max normalization [eq. (1)] is chosen. It rescales the features of neural network to a new range, the underlying distribution of the features remaining unchanged:

$$x_{norm} = \min_t + (\max_t - \min_t)\frac{x\text{-min}}{\max - \min} \quad (1)$$

where min_t and max_t are the minimum and maximum values of the range which is -0.9 and 0.9, respectively. *Min* and *max* are the limits of the interval in which the feature x can take values.

Process Modeling with ANN-DE Tool

In order to model the process, a methodology based on a hybrid combination of DE and ANN was applied. The algorithm, called hSADE-NN, was proposed in one of our previous works[42] and consists in employing, along DE and ANN, two other algorithms (Random Search - RS and Back Propagation - BK). The role of RS and BK is to locally improve the best solutions found at each generation, and therefore to improve the performance of the overall algorithm. Two local algorithms were applied instead of only one because it was observed that, in some cases, BK alone does not manage to improve the solutions.

The role of the ANN is to model the process, while DE acts as a model optimizer. Among the existing types of ANNs, the variant chosen in this work is represented by the feed-forward multilayer perceptron neural network (MLP). The main aspects taking into consideration when selecting MLP are related to its simple structure, easy implementation, and property of universal approximator. Since it was determined that a network with enough neurons in a single hidden layer can model any type of function,[43] a limitation to the number of hidden layers was imposed at two. Also, a maximum number of neurons in the hidden layers was set up (30) as this has an impact on overall algorithm performance because a big ANN translates into a lengthy individual for the optimization procedure. This correlation is due to the fact that the evolutionary process of DE is applied to a population of individuals which represents encoded potential neural models for the considered process.

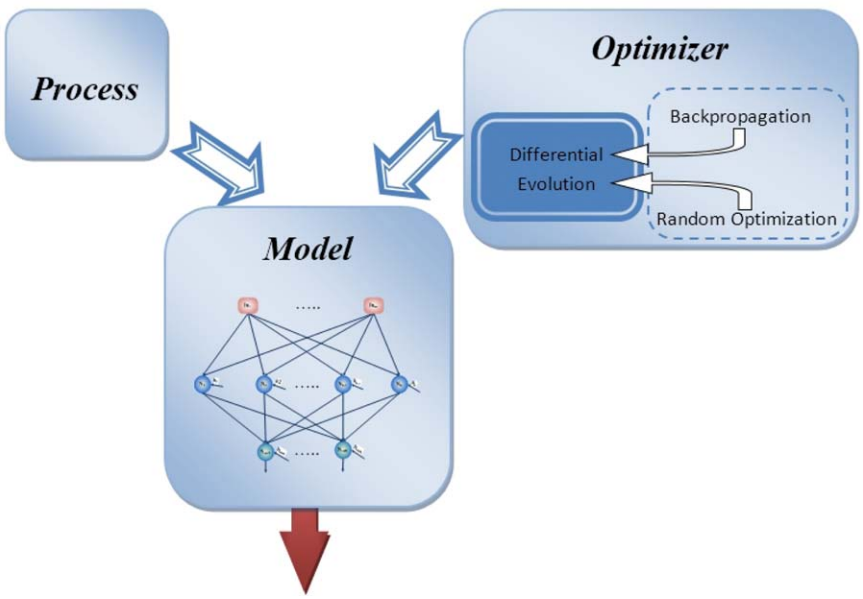

Figure 3. Graphical representation of the methodology applied to model the process. [Color figure can be viewed in the online issue, which is available at wileyonlinelibrary.com.]

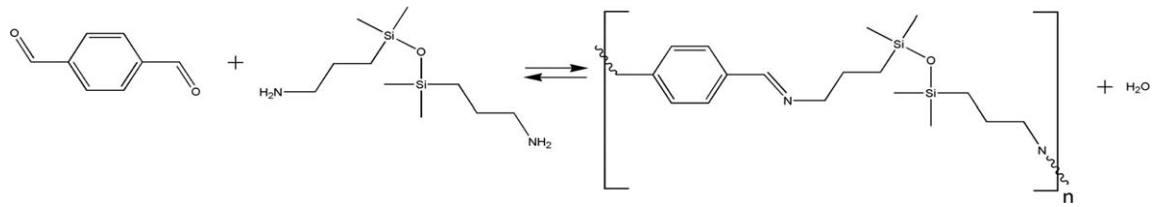

Figure 4. Reaction pathway leading to polyazomethine.

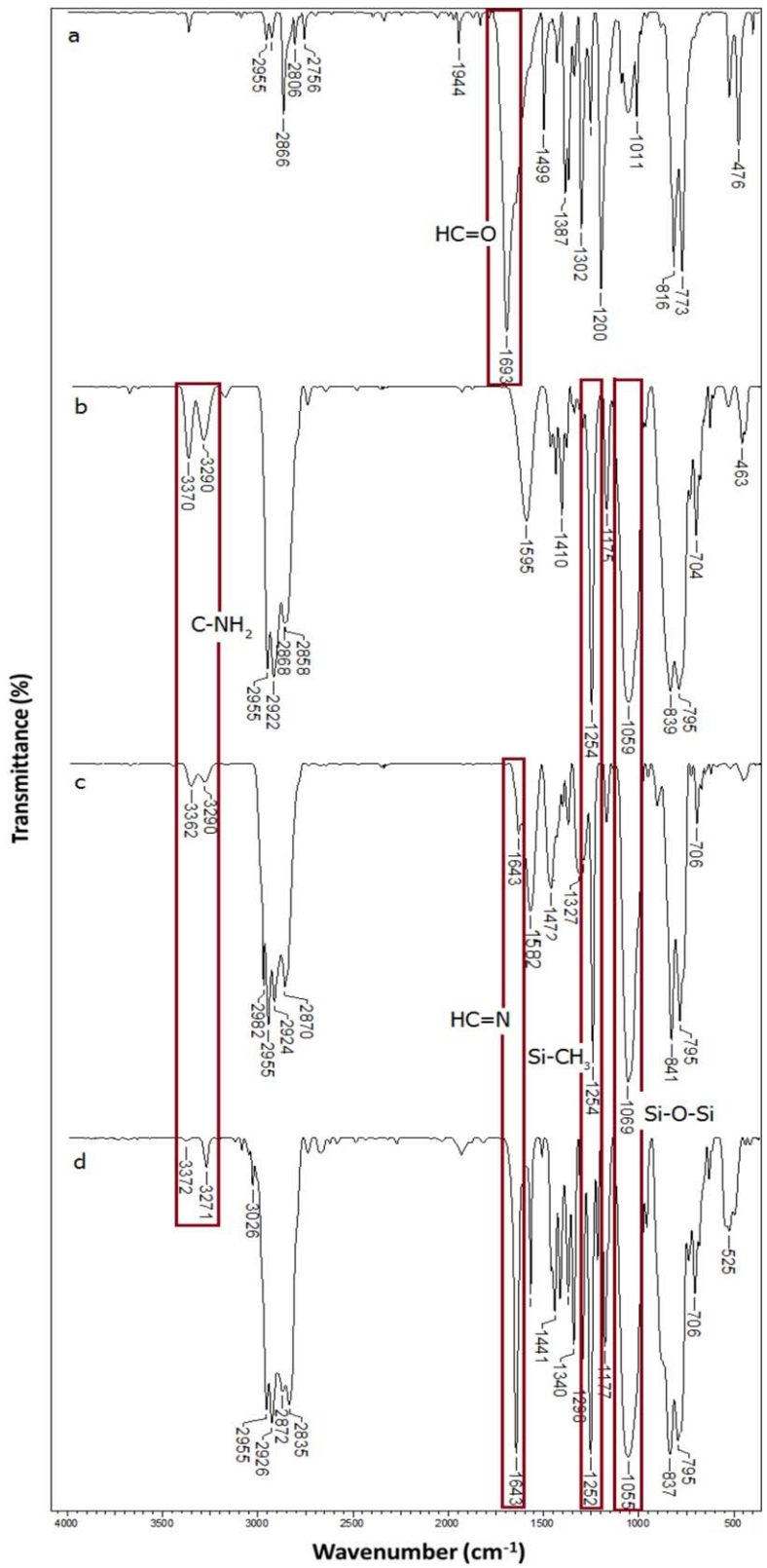

Figure 5. Comparative IR spectra: (a) AT; (b) AP0; (c) AT partially converted in azomethine; (d) siloxane-ftalimine polyazomethine (0.7 g AT, 1.14 mL AP0 and 6.56 mL THF at 25°C). [Color figure can be viewed in the online issue, which is available at wileyonlinelibrary.com.]

Table II. Top 10 Results (Neural Models) Obtained with the hSADE-NN Algorithm

No.	Fitness	MSE train	$R^2_{training}$	RMSE	MSE test	$R^2_{testing}$	RMSE	Topology
1	1755.002	0.000570	0.97123	0.2555	0.000688	0.98291	0.18159	5 : 20 : 1
2	1741.441	0.000574	0.97078	0.2575	0.000703	0.98217	0.18556	5 : 17 : 1
3	1733.064	0.000577	0.97043	0.2587	0.000704	0.98211	0.18563	5 : 18 : 1
4	1726.380	0.000579	0.97021	0.2597	0.000721	0.98125	0.19011	5 : 20 : 1
5	1731.415	0.000578	0.97041	0.2590	0.000725	0.98100	0.19133	5 : 17 : 1
6	1717.01	0.000582	0.96991	0.2611	0.000730	0.98074	0.19272	5 : 14 : 1
7	1730.213	0.000578	0.97036	0.2591	0.000731	0.98070	0.19284	5 : 8 : 1
8	1690.215	0.000592	0.96891	0.2653	0.000733	0.98062	0.19337	5 : 10 : 1
9	1702.381	0.000587	0.96935	0.2634	0.000737	0.98045	0.19440	5 : 3 : 1
10	1624.692	0.000616	0.97123	0.2555	0.000738	0.98291	0.18159	5 : 10 : 1

An encoding procedure was applied because DE cannot work with ANN in its natural state. Since the fitness function and BK algorithm can only be employed on ANN structures and not on DE individuals, a simple direct encoding/decoding step is performed every time the situation requires it.

As mentioned previously, DE automatically evolves a set of ANNs in order to determine their internal parameters and topology. The evolutionary process starts with a pool of randomly generated solutions (improved with the Opposition Based Learning approach - OBL) and stops until a termination criterion is reached. OBL is based on the idea that, when randomly generating a solution, the probability that its opposite is closer to the desired solution is 50%. Consequently, the OBL application on the initialization procedure reduces the distance between the generated solutions and the desired ones, improving the probability of finding suitable models.

The stop criterion is formed from the combination of the low Mean Squared Error (MSE) value, equal to e^{-10}, or the number of generation being equal to a predefined value. In order to eliminate the need of manually fine-tune of the DE parameters, a self-adaptive procedure is applied for the crossover factor (Cr) and for the mutation factor (F), which are the control parameters of the algorithm. On the other hand, the number of individuals in the population Np (which represents the third DE control parameter) is set fixed and equal to 250. This value was selected based on observations from a set of preliminary simulations (MSE variation with the number of generations), indicating that this is a good trade-of between performance and resources consumed.

At the end of each generation, the best solution from the pool of potential ones is chosen, meaning the solution with the highest fitness (which is inversely proportional with the MSE in the

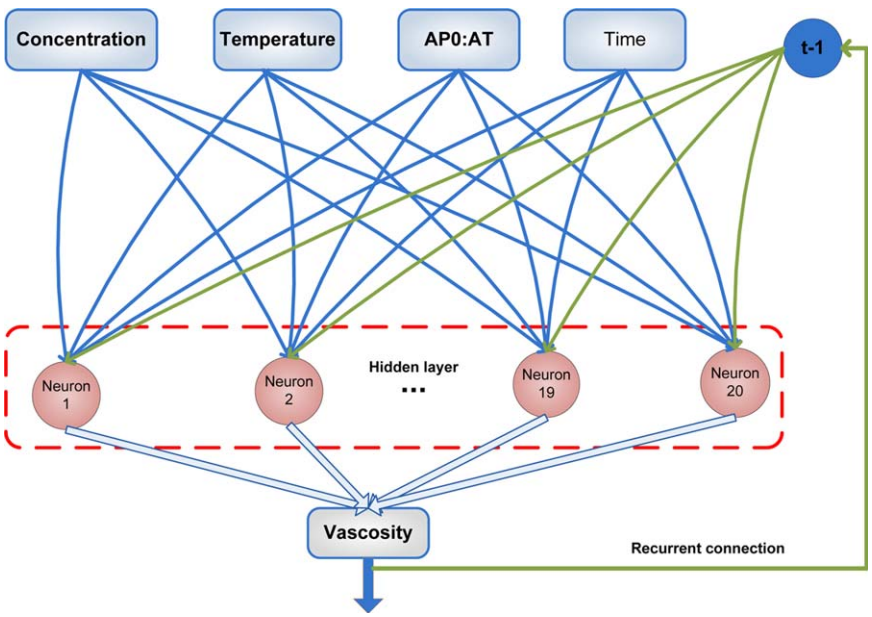

Figure 6. Structure of the obtained ANN model. [Color figure can be viewed in the online issue, which is available at wileyonlinelibrary.com.]

training phase as described by Eq. (2)). In order to improve it further, based on a random approach, either BK or RS is applied to perform a local search, the best solution being replaced only when a better individual is found.

$$fitness = \frac{1}{MSE_{training} + e^{-10}} \quad (2)$$

A simplified schema of the modeling procedure and how it is applied to the approached process is presented in Figure 3. Based on the experimental data gathered from the process, a series of ANN models are generated and improved with DE algorithm hybridized with BK and RS. In the end, the best solution (chosen based on its fitness value) is used for generating predictions useful for the chemical engineer.

RESULTS AND DISCUSSION

Experimental Results

The reaction between terephthalic aldehyde and 1,3-bis(3-aminopropyl) tetramethyldisiloxane, leading to the formation of polyazomethine, is presented in Figure 4. The reaction was performed in solution by using THF as a solvent, in the absence of any catalyst.

The reaction carrying out with the formation of azomethine group was verified by FT-IR spectroscopy (Figure 5) following the disappearance of the band at 1693 cm^{-1} corresponding to carbonylic bond and the bands of the amine bond's at 3270 and 3372 cm^{-1}, which lead to the development of the band at 1643 cm^{-1} assigned to new formed azomethine group. The presence of Si—O—Si bond is proved by the strong band at 1055–1069 cm^{-1}, while Si-CH_3 groups manifested by the absorption band at 1252–1254 cm^{-1}.

Modeling Results

After the data were gathered and processed, a set of simulations with the hSADE-NN algorithm were performed. Initially, four inputs were considered, represented by the following parameters: *C*, *T*, *AP0* : *AT*, and time, *t*, and an output - viscosity. Depending on the initial conditions, the dynamic of the system varies considerably and the simulations results were not acceptable. Although MSE had relatively good values (2×10^{-3}–5×10^{-3}), when comparing the dynamic of the process it was observed that the differences were quite high. Since the modeling scope was to determine a model positioned in the minimum area of the search space, a 5th input for the model was introduced in the form of a recurrence, respectively, the viscosity at a previous time. In this manner, the output of the model at a specific moment of time *t* has an influence on the predictions at the next moment ($t + 1$). In this case, the type of ANN was kept the same (MLP), the number of inputs is raised to five and the recurrence is simulated by applying a data processing technique.

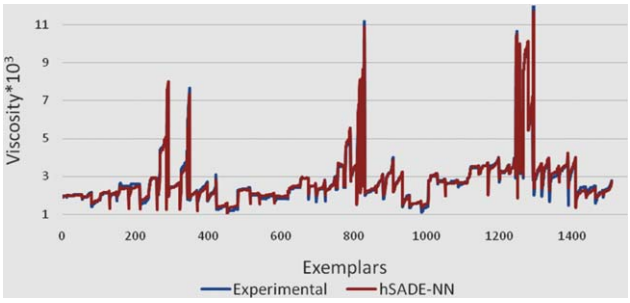

Figure 7. Comparison between experimental data and neural network predictions for the best model, MLP(5 : 20 : 1) in the testing phase. [Color figure can be viewed in the online issue, which is available at wileyonlinelibrary.com.]

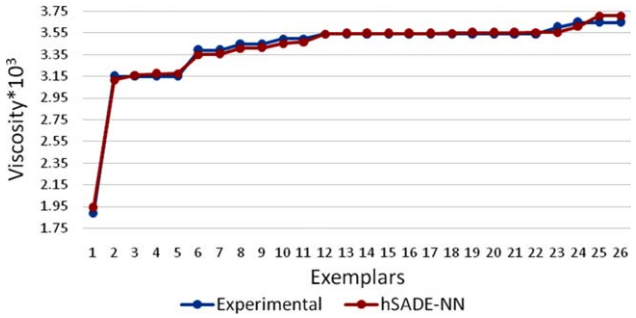

Figure 8. Experimental vs. predictions with hSADE-NN for $C = 25\%$, $T = 30°C$, AP0/AT = 3 : 4. [Color figure can be viewed in the online issue, which is available at wileyonlinelibrary.com.]

As previously discussed, a series of limitations to the network topologies were imposed, the maximum number of allowed neurons in the hidden layer being 30. The top 10 neural models obtained are listed in Table II, where the topology is denoted as "*inputs: hidden neurons: outputs*", MSE represents the mean squared error, R^2 is the coefficient of determination (computed as the correlation raised to the power of two) and RMSE is the root mean squared error. The fitness is computed based on MSE in the training phase and it is internally used by the algorithm for determining the performance of the generated models. The MSE in the testing phase was not included in the fitness function in order to have an external dataset to the model determination.

Considering that the best model is the one with the lowest MSE in the testing phase, from Table II it can be seen that the network (5 : 20 : 1) with a MSE of 0.00068 is the best (Figure 6). This model has a correlation of 0.9855 in the training phase and 0.9914 in the testing phase. A comparison between the experimental data and the predictions of this ANN for data unseen in the training phase is presented in Figure 7.

The differences between the predicted data and the experimental one (for the entire dataset) are small, fact which points out that the considered approach is able to efficiently model the process. When comparing the dynamic of the system (experimental vs. predictions), the differences are also quite small, as Figure 8 shows.

The neural network model proved capable to process a substantial amount of data and gives almost overlapping predictions with the experimental data.

The procedure applied here is not dependent of the polyazomethine synthesis process. Thus, based on its general character, the developed modeling and optimization technique has good chances to successfully be applied to other polymerization processes.

CONCLUSIONS

The formation of an alternant siloxane-organic polyazomethine was monitored indirectly while pursuing viscosity change, *in situ*, by using an automatic viscometer. A series of syntheses were performed, using different concentrations, monomers ratios, or temperatures, in a 10,800 seconds interval. The reaction occurrence was also qualitatively verified by FTIR spectrometry. The high number of data obtained was processed using a simple algorithm procedure. In this manner only the relevant information about the process was retained.

The considered process was also modeled using two bio-inspired computing techniques: ANN and DE. The ANN acts as a model, while DE is the optimizer employed to simultaneously perform a topological and parametric optimization of the neural network model. The good results obtained (good performance measures, small overall differences and good correlation between experimental data and model predictions in what concerns the dynamic of the process) indicate that the considered modeling approach is able to efficiently determine accurate models for the synthesis process of polyazomethine. In addition, the obtained predictions are useful for a significant understanding of the process, providing information on the whole investigated domain and saving, in this manner, materials, energy, and time.

ACKNOWLEDGMENTS

This work was supported by the "Partnership in priority areas–PN-II" program, financed by ANCS, CNDI - UEFISCDI, project PN-II-PT-PCCA-2011-3.2-0732, No. 23/2012.

REFERENCES

1. Burroughes, J. H.; Bradley, D. D. C.; Brown, A. R.; Marks, R. N.; Mackay, K.; Friend, R. H.; Burn, P. L.; Holmes, A. B. *Nature* **1990**, *348*, 352.
2. Lashanizadegan, M.; Sarkheil, M. *J. Serbian Chem. Soc.* **2012**, *77*, 1589.
3. Marin, L.; Cozan, V.; Bruma, M. *Polym. Adv. Technol.* **2006**, *17*, 664.
4. Marin, L.; Cozan, V. *Mem. Sci. Sect. Rom. Acad. Ser. IV* **2010**, *33*, 35.
5. Sek, D.; Grucela-Zajac, M.; Krompiec, M.; Janeczek, H.; Schab-Balcerzak, E. *Opt. Mater.* **2012**, *34*, 1333.
6. Tuncel, M.; Ozbulbul, A.; Seri n, S. *React. Funct. Polym.* **2008**, *68*, 292.
7. Catanescu, O.; Grigoras, M.; Colotin, G.; Dobreanu, A.; Hurduc, N.; Simionescu, C. I. *Eur. Polym. J.* **2001**, *37*, 2213.
8. Mahnaz, S.; Ali, A. E. *Iran. Polym. J.* **2003**, *12*, 43.
9. Hussein, M. A.; Abdel-Rahman, M. A.; Geies, A. A. *J. Appl. Polym. Sci* **2012**, *126*, 2.
10. Sek, D.; Jarzabek, B.; Grabiec, E.; Kaczmarczyk, B.; Janeczek, H.; Sikora, A.; Hreniak, A.; Palewicz, M.; Lapkowski, M.; Karon, K.; Iwan, A. *Synth. Metals* **2010**, *160*, 2065.
11. Anant, P.; Devjani, A. *Int. J. ChemTech Res.* **2011**, *3*, 1891.
12. Niu, H.; Kang, H.; Cai, J.; Wang, C.; Bai, X.; Wang, W. *Polym. Chem.* **2011**, *2*, 2804.
13. Grigoras, M.; Antonoaia, N. C. *Eur. Polym. J.* **2005**, *41*, 1079.
14. More, A. S.; Sane, P. S.; Patil, A. S.; Wadgaonkar, P. P. *Polym. Degrad. Stab.* **2010**, *95*, 1727.
15. Gonzaga, J. C. B.; Meleiro, L. A. C.; Kiang, C.; Maciel Filho, R. *Comput. Chem. Eng.* **2009**, *33*, 43.
16. Sadavarte, N. V.; Avadhani, C. V.; Wadgaonkar, P. P. *High Perform. Polym.* **2011**, *23*, 494.
17. Marin, L.; Cozan, V.; Bruma, M. *Polym. Adv. Technol.* **2006**, *17*, 664.
18. Farcas, A.; Harabagiu, V. *Rev. Roum. Chim.* **2007**, *52*, 887.
19. Iwan, A.; Schab-Balcerzak, E.; Pociecha, D.; Krompiec, M.; Grucela, M.; Bilski, P.; Kłéosowski, M.; Janeczek, H. *Opt. Mater.* **2011**, *34*, 61.
20. Madec, P. J.; Peres, R.; Marechal, E. *Makromol. Chem. Macromol. Symp.* **1991**, *47*, 357.
21. Racles, C.; Cazacu, M.; Vasiliu, M.; Cozan, V. *Polym. Plast. Technol. Eng.* **2005**, *44*, 1049.
22. Racles, C.; Cozan, V.; Cazacu, M.; Foldes, E.; Sajo, I. *High Perform. Polym.* **2002**, *14*, 397.
23. Cazacu, M.; Vlad, A.; Munteanu, G.; Airinei, A. *J. Polym. Sci. A Polym. Chem.* **2008**, *46*, 1862.
24. Vlad, A.; Cazacu, M.; Munteanu, G.; Airinei, A.; Budrugeac, P. *Eur. Polym. J.* **2008**, *44*, 2668.
25. Zaltariov, M.-F.; Cazacu, M.; Racles, C.; Musteata, V.; Vlad, A.; Airinei, A. *J. Appl. Polym. Sci* **2015**, to appear. DOI: 10.1002/APP.41631.
26. Vacareanu, L.; Ivan, T.; Grigoras, M. *High Perform. Polym.* **2012**, *24*, 717.
27. Khalil, R. A.; Jalil, A. H.; Abd-Alrazzak, A. Y. *JICS* **2009**, *6*, 345.
28. Guillermo, O. **2012**, Available at: http://www.uel.br/pos/bioenergia/arquivos/material/guillermo_orellana/optodes_for_process_analysis_orellana.pdf.
29. Malkin, A. Ya.; Kilicjikhin, S. G. In Rheokinetics: Rheological Transformations in Synthesis and Reactions of Oligomers and Polymers; Wiley: New York, **2008**.
30. Subudhi, B.; Jena, D. *Appl. Soft Comput.* **2011**, *11*, 861.
31. Noor, R. A. M.; Ahmad, Z.; Don, M. M.; Uzir, M. H. *Can. J. Chem. Eng.* **2010**, *88*, 1065.
32. Curteanu, S. *Centr. Eur. J. Chem.* **2004**, *2*, 113.
33. Gonzaga, J. C. B.; Meleiro, L. A. C.; Kiang, C.; Maciel Filho, R. *Comput. Chem. Eng.* **2009**, *33*, 43.
34. Contant, S.; Mesa, P. V. R.; Lona, L. M. F. **2005**, 2nd Mercosur Congress on Chemical Engineering. 4th Mercosur Congress on Process System Engineering. Availabe at: http://www.enpromer2005.eq.ufrj.br/nukleo/pdfs/0204_lona_enpromer.pdf.
35. Fernandes, F. A. N. *J. Appl. Polym. Sci.* **2005**, *98*, 2088.
36. Curteanu, S.; Leon, F.; Furtuna, R.; Dragoi, E. N.; Curteanu, N. The 2010 International Joint Conference on Neural Networks (IJCNN), 18–23 July, **2010**, p 1, Barcelona, Spain.

37. Leite, M. S.; Dos Santos, B. F.; Lona, L. M. F.; Da Silva, F. V.; Frattini Fileti, A. M. *Chem. Eng. Trans.* **2011**, *24* 385.

38. Salman, A.; Engelbrecht, A. P.; Omran, M. G. H. *Eur. J. Oper. Res.* **2007**, *183*, 785.

39. Feoktistov, V. In Differential Evolution: in Search of Solutions; Springer: Berlin, **2006**.

40. Babu, B. V.; Chakole, P. G.; Syed Mubeen, J. H. *Chem. Eng. Sci.* **2005**, *60*, 4822.

41. Gujarathi, A. M.; Babu, B. V. *Chem. Eng. Sci.* **2010**, *65*, 2009.

42. Curteanu, S.; Suditu, G.; Buburuzan, A. M.; Dragoi, E. N. *Environ. Sci. Pollut. Res.* **2014**, 1.

43. Hornik, K.; Stinchcombe, M.; White, H. *Neural Networks* **1989**, *2*, 359.